Chemistry & Biology
Article

Rational Development of Caged-Biotin Protein-Labeling Agents and Some Applications in Live Cells

Takuya Terai,[1,2] Eri Maki,[1,2] Shigeru Sugiyama,[2,3] Yoshinori Takahashi,[2,3] Hiroyoshi Matsumura,[2,3,4] Yusuke Mori,[2,3,4] and Tetsuo Nagano[1,2,*]
[1]Graduate School of Pharmaceutical Sciences, The University of Tokyo, 7-3-1 Hongo, Bunkyo-ku, Tokyo 113-0033, Japan
[2]CREST, JST, Sanbancho-blg, 5 Sanbancho, Chiyoda-ku, Tokyo, 102-0075, Japan
[3]Graduate School of Engineering, Osaka University, 2-1 Yamadaoka, Suita, Osaka 565-0871, Japan
[4]SOSHO Inc., 1-6-18 Motomachi, Chuo-ku, Osaka 541-0053, Japan
*Correspondence: tlong@mol.f.u-tokyo.ac.jp
DOI 10.1016/j.chembiol.2011.09.007

SUMMARY

Biotin-(strept)avidin complex is widely used in biotechnology because of its extremely high binding constant, but there is no report describing spatiotemporally controlled formation of the complex in live cells. Here, based on X-ray crystal structure analysis and calorimetric data, we designed and synthesized photoreleasable biotins, which show greatly reduced affinity for (strept)avidin, but recover native affinity after UV irradiation. For application at the cell surface, we introduced an amine-reactive moiety into these "caged" biotin molecules. Specific fluorescence imaging of live cells that had been labeled with these agents and then UV-irradiated, was accomplished by addition of streptavidin conjugated with a fluorophore. We also demonstrated the applicability of these compounds for UV-irradiated-cell-specific drug delivery by using caged-biotin-labeled cells, a prodrug, and streptavidin conjugated with a prodrug-activating enzyme.

INTRODUCTION

Biotin is a water-soluble small molecule (MW 244) that works as a cofactor for several carboxylases (Figure 1A). Although the biological functions and biosynthetic pathway of biotin are still under investigation (Stanley et al., 2001; Lin et al., 2010), biotin is one of the most widely used molecules in biotechnology, in combination with its partner protein, (strept)avidin. Avidin is a tetrameric and basic (p*I* ~10) glycoprotein found in egg white, consisting of 128 amino acids per subunit. Streptavidin, which is also a tetrameric protein isolated from *Streptomyces avidinii,* does not possess a sugar moiety and its isoelectric point is near neutral, resulting in less nonspecific binding to other molecules. The physiological roles of these proteins are not well known, but it is thought that they act as a defense against bacteria by inactivating bacterial enzymes that require biotin as a cofactor (Diamandis and Christopoulos, 1991).

Biotin-(strept)avidin complex is extensively used in the life sciences. In fact, biotinylation of DNAs, proteins, and other biomolecules is the first choice for separation or visualization of the molecules themselves or their binding partners (Wilchek and Bayer, 1988; McMahon, 2008). The reasons why the biotin-avidin complex has been so widely used are that the complex has an extremely high affinity (Ka ~10^{15} M^{-1}) and that the complex formation is nearly unaffected by pH, temperature, organic solvents, or denaturing agents (Sakahara and Saga, 1999; Green, 1963). In addition, the tetrameric structure of avidin allows it to bind simultaneously to biotin groups on the target and to other biotinylated molecules, such as reporter enzymes. This multiple binding property readily allows for signal amplification, which provides increased sensitivity. Notably, in all of these applications, the carboxyl group of the biotin side chain is chemically linked to biological molecules, and the complex between the biotin derivatives and (strept)avidin is formed immediately upon addition of the protein (Yamaguchi et al., 2010). In other words, the formation of the complex is automatic and depends only on the presence of the two molecules.

On the other hand, a few researchers have controlled this complex formation in a stimulus-responsive manner by chemical modification of biotin, mainly in order to site-specifically immobilize proteins while retaining their biological activities (Lee et al., 2002; Hengsakul and Cass, 1996). This was done by precoating the surface of a chip with deactivated biotin containing a photolabile protecting group (Sundberg et al., 1995; Pirrung and Huang, 1996), or an electrochemically removable protecting group (Kim et al., 2004); these intentionally deactivated biotin derivatives are called caged biotins in this paper due to the conceptual analogy with caged biomolecules (Ellis-Davies, 2007), such as caged glutamate and caged ATP. Subsequently, selected sites of the chip are activated by irradiation through a photo mask or by electrochemical perturbation; then the surface is exposed to a solution of a target protein labeled with avidin to be immobilized on the activated sites. In these reports, however, although the methodology appears general, neither any application of the caged biotins to live cells, nor detailed structural and thermodynamical analysis of the complexes between caged biotins and avidin was described. Considering that the biotin-avidin complex is widely used in biochemistry, either in vitro or in cell culture, we thought that it would be very useful to extend the range of application of caged biotins to live cells.

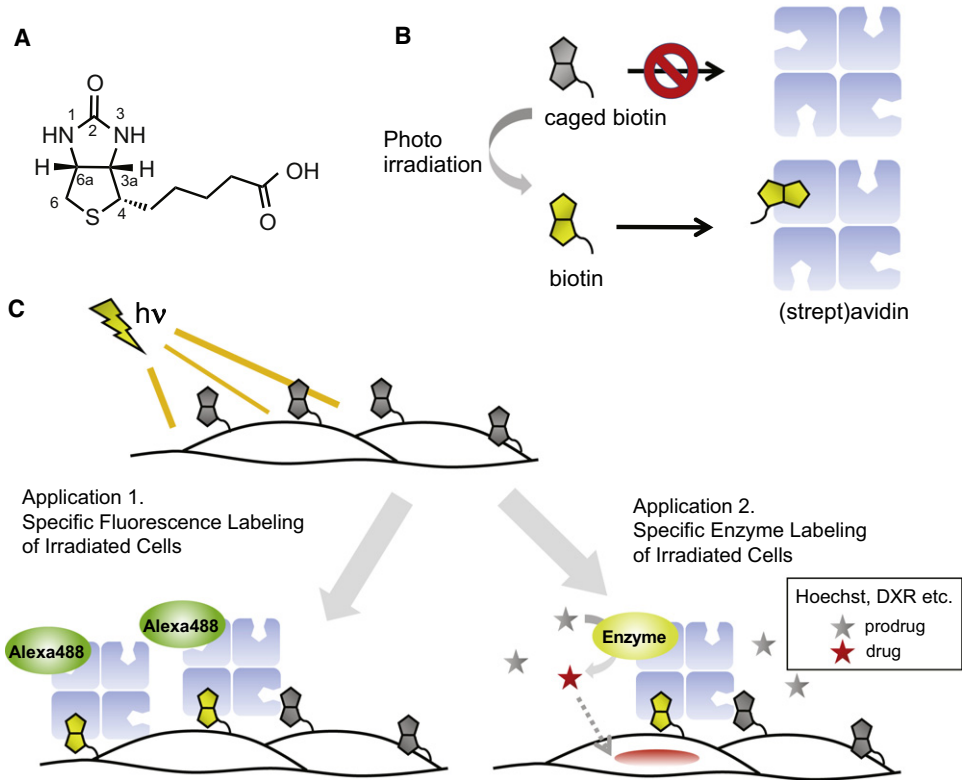

Figure 1. Schematic Illustration of Caged Biotin and Some of Its Applications

(A) Chemical structure of biotin.

(B) Conceptual illustration of caged biotin. Caged biotin can strongly bind to (strept)avidin only after photoirradiation.

(C) Strategy for specific fluorescence labeling of irradiated cells by use of streptavidin conjugated with a fluorophore and pretargeted caged biotin (application 1), and for irradiated-cell-specific drug delivery by combined use of a prodrug, streptavidin conjugated with an enzyme, and pretargeted caged biotin (application 2).

Therefore, in this study, we aimed to rationally design caged biotin-(strept)avidin complexes that could be used in live cells. Based on structural information about the essential structure of biotin for protein binding, we synthesized model compounds modified at the urea nitrogen. All of them had remarkably lower binding constants than the parent compound. Encouraged by these results, we developed photoactivatable caged biotin derivatives that were modified with photocleavable groups at the urea nitrogen, and showed that they recovered the original binding affinity for avidin after UV irradiation (Figure 1B). We then designed and synthesized novel caged biotin derivatives that could label lysine residues of cell-surface proteins. To confirm the utility of these compounds, we performed three experiments, i.e., specific cell-surface fluorescence labeling, enzyme-mediated nuclear staining, and prodrug-dependent killing of UV-irradiated cells labeled with the synthesized compounds, using streptavidin conjugated to a fluorophore or a hydrolytic enzyme. These experiments are illustrated schematically in Figure 1C.

RESULTS

Biotin Derivatives Modified at the Urea Moiety

For rational development of caged biotins, it is important to know which part of the biotin structure is essential for the affinity. First, we considered this point based on the results of X-ray crystallography of biotin-avidin complex (Pugliese et al., 1993). Figure 2A is a magnified view of the biotin-binding pocket of the complex, showing biotin as a ball and stick model. The interaction of the ligand and the protein was analyzed by Molegro Molecular Viewer software (Molegro ApS, Denmark), and the contribution of each atom to the total stabilization energy was evaluated. Namely, the size of the ball corresponds to the importance of the atom for the affinity. The N′-1 urea nitrogen (yellow arrowhead), in addition to urea oxygen, was suggested to be the most important, while N′-3 nitrogen, the methylene linker of the pentanoic acid moiety, and sulfur atom appeared not to play major roles. Also, although the carboxylic acid moiety forms hydrogen bonds with protein amino acids, modification to amide or ester has little effect on the binding affinity (Sugawara et al., 1997). Considering the synthetic difficulty of modifying urea oxygen, we decided to introduce substituents at the N′-1 position to block the affinity of biotin for (strept)avidin.

As model compounds, we designed and synthesized three biotin derivatives with acetyl and alkyl groups at N′-1 (Figure 2B): monoAc-biotin, monoZ-biotin, and diMe-biotin (see Supplemental Experimental Procedures, available online, for synthetic details). We then determined the binding constants (K_a) of the derivatives with avidin by means of isothermal titration calorimetry (ITC) (Figure 2C). Indeed, the K_a values of the

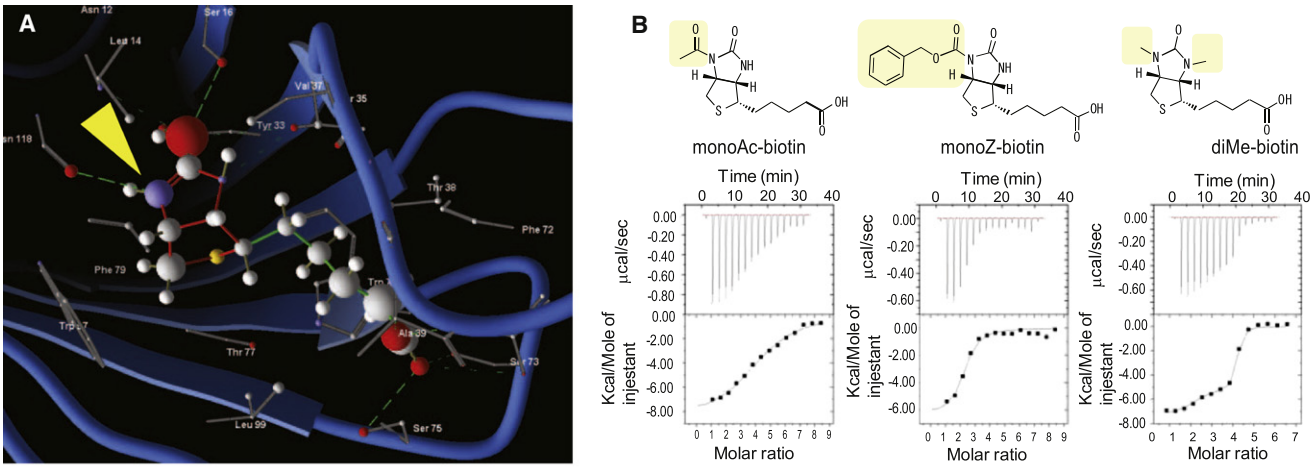

C

	N	K_a (M^{-1})	ΔH (cal/mol)	ΔS (cal/mol/deg)
monoAc-biotin	4.0	2.0×10^5	-7.2×10^4	0.49
monoZ-biotin	2.0	2.3×10^6	-8.4×10^3	1.3
diMe-biotin	2.1	5.5×10^6	-6.1×10^3	11
	1.7	4.0×10^8	-6.3×10^3	18

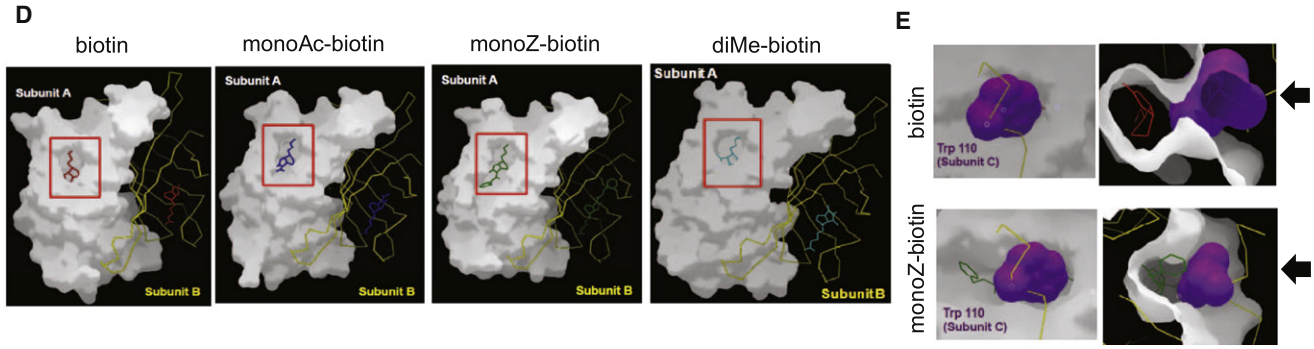

Figure 2. The Effect of Introduction of Alkyl and Acetyl Groups at the Urea Moiety of Biotin

(A) Interaction between biotin and avidin. The biotin-binding pocket of avidin is shown in detail. The crystal structure was derived from Protein Data Bank 1AVD, and analyzed by Molegro software. In this figure, carbon is shown in white, oxygen in red, nitrogen in blue, and sulfur in yellow. The yellow arrowhead indicates the N′-1 position, and green dotted lines indicate hydrogen bonds.

(B) ITC experiments on biotin derivatives with modified urea moieties. Heat effects were recorded as a function of time during 15 successive 2 µl injections of 800 µM solution of monoAc-biotin, monoZ-biotin or diMe-biotin into the cell containing either 15 µM solution of avidin or buffer solution. Buffer conditions: 0.1 M sodium phosphate, 0.4% DMSO (pH 7.4).

(C) Thermodynamic parameters of biotin derivatives modified at the urea moiety, determined by ITC.

(D) Overall structures of the complexes between biotin derivatives and avidin. In these figures, avidin subunit A is shown in white as a space-filling model, and subunit B in yellow as a wire model of central carbon atoms. The biotin-binding pocket is highlighted by a red square.

(E) Closeup view of the interface between subunits A and C. Subunit C is shown in yellow as a wire model of central carbon atoms. Trp110 of subunit C is shown in purple. Biotin is shown in red stick and avidin is shown as a semitransparent surface. The black arrow in the right figure indicates the direction of viewpoint of the left figure. See also Figures S1 and S2 and Table S1.

complexes were dramatically decreased (monoZ-biotin 2.3 × 10^6 M^{-1}, monoAc-biotin 2.0 × 10^5 M^{-1}, diMe-biotin 5.5 × 10^6 M^{-1} and 4.0 × 10^8 M^{-1}, respectively), being as much as 10^9∼10^{10}-fold lower than that of the native complex. Curiously, the number of binding sites of monoZ-biotin to avidin tetramer was two, whereas the number in the case of other derivatives, including native biotin itself, was four. Furthermore, unlike the other compounds, diMe-biotin bound to avidin in two steps, implying the presence of two different binding sites. The results suggested the possibility that the overall protein conformation might be altered by ligand binding, or that these ligands bind to avidin at different sites from the biotin-binding pocket. To address these questions, we crystallized the complexes from sodium-citrate buffer containing ammonium sulfate (Figure 2D; see also Table S1; Figures S1 and S2A–S2D). Notably, we found that the microstirring technique improved the quality of the

crystals. We shook the sitting-drop vapor-diffusion crystallization plates with a rotating shaker at 50 rpm (Adachi et al., 2004; Shimizu et al., 2009). As shown in Figure 2D, the binding sites of all the biotin derivatives were the same as that of biotin, thus excluding the second possibility. Also, the position of the main carbon chain of avidin in these complexes was almost the same as that of biotin-avidin complex. When the binding site was magnified, however, it was clear that the binding pocket in avidin was larger in the complexes of the novel derivatives, in particular monoZ-biotin, than in the case of biotin. This was due to the movement of protein side chains so as to accommodate bulky substituents in the pocket, which resulted not only in reorganization of the delicate hydrogen-bonding network of the native complex (Pazy et al., 2002), but also in weaker hydrophobic interactions between these biotin derivatives and aromatic residues of the protein. Especially, Trp110 of the adjacent subunit, the residue that plays a pivotal role in stabilizing the tetrameric structure of the complex (Laitinen et al., 1999; Laitinen et al., 2003), was not able to completely occupy the space formed at the biotin pocket (Figure 2E). In this sense, the crystal structures explain the significantly lower K_a values of biotin derivatives with avidin. However, in contrast to the results of ITC, all the biotin derivatives bound to the protein with a stoichiometry of 4:1. Although further investigation is necessary, the discrepancy may be attributed to the difference between the experimental conditions of ITC and those of X-ray crystallography, such as buffer composition and protein concentration. Another possibility is that the results of ITC reflect the kinetics of the binding, that is, only the first two monoZ-biotin molecules bind rapidly to the protein, followed by slow conformational change that allows for the binding of the other two.

Fluorescence polarization (FP) assay was also carried out to obtain information about the binding sites. To measure FP, we synthesized biotin derivatives that were conjugated with a fluorophore at the carboxylate moiety through a short linker (see Supplemental Experimental Procedures for synthetic details). The value of FP was clearly increased when avidin was added to solutions of the biotin derivatives, corresponding to the protein binding of the derivatives (Figure S2E). Importantly, the value decreased to the original level when excess native biotin was added to the assay mixture. The data indicated that the biotin derivatives bind to the same biotin pocket in avidin as native biotin, even though the binding constants were much lower.

Taken together, these results demonstrate for the first time that modification at the biotin urea moiety can reduce the affinity for avidin by approximately $10^9 \sim 10^{10}$ fold. So, modification at this site should be widely available to design biotin derivatives that do not bind to avidin.

Development of Caged Biotins

We next designed and synthesized two photoactivatable biotin derivatives: NPC-biotin and DMNPE-biotin (Figure 3A; see Supplemental Experimental Procedures for synthetic details), which were expected to exhibit a drastic increase of binding constant upon photoirradiation, owing to release of native biotin (Sundberg et al., 1995). These compounds consist of biotin and a nitrobenzyl-based photo-removable protecting group that can be excited at 365 nm with a high uncaging rate and a high photolysis quantum yield (Gee et al., 1998). First, to confirm photorelease of biotin, HPLC analysis of NPC-biotin was performed before and after photo-irradiation (365 nm, 20 min, 2.8 mW/cm^2). Under this condition, conversion of the starting compound to the expected product proceeded smoothly without any apparent by-product formation; the reaction yield was approximately 90% (Figure S3A). We next determined the K_a values of the derivatives and avidin by ITC (Figures 3B–3D). As expected, the K_a values of the complexes were drastically decreased (NPC-biotin: 1.5×10^4 M^{-1}, DMNPE-biotin: 1.3×10^4 M^{-1}) compared with that of native biotin. Moreover the binding constant of the two derivatives to avidin recovered to the value of native biotin after photoirradiation. Note that the number of binding sites of caged biotin after photoirradiation was estimated to be somewhat higher than that of native complex because a small amount of the starting compound was still present in the mixture.

To probe the structural details of the interaction between caged biotin and avidin, we solved the structure of the avidin complex with NPC-biotin at 2.0 Å resolution (Table S1; Figures S1 and S3B). Consistent with the results in the previous section, the overall binding mode of NPC-biotin was similar to that of biotin, with Trp110 in the neighboring subunit partially interacting with the biotin pocket (Figure 3E). The biotin pocket was also expanded to approximately the same size as that in the case of monoZ-biotin, and the bulky protecting group inhibited both the hydrophobic and hydrogen-bonding interactions between the ligand and the protein.

Specific Fluorescence Labeling of Irradiated Cells

As the first application of these caged biotins in live cells, we devised a method for specific fluorescence labeling of irradiated cells by combined use of fluorophore-conjugated streptavidin and pretargeted caged biotin. First, as illustrated in Figure 4A, proteins on the cell surface are labeled with caged biotin via a covalent amide bond. Then the target cells are UV irradiated, followed by the addition of fluorophore-conjugated streptavidin. Only at the site of irradiation, where the strong affinity of native biotin is recovered as a result of uncaging, should the fluorescence of streptavidin be detected. To realize this strategy, we designed and synthesized amine-reactive caged biotins, NPC-biotin-linker-SE and DMNPE-biotin-linker-SE (Figure 4A; see Supplemental Experimental Procedures for synthetic details). In these compounds, succinimidyl ester was introduced as a reactive moiety able to form a covalent bond with the amino group of lysine residues of the surface proteins. The compounds were loaded into cultured HeLa cells, and 30 min later, the cells were irradiated and mixed with streptavidin conjugated with AlexaFluor488. Unbound streptavidin was washed out before imaging. As shown in Figure 4B, a strong fluorescence signal was only observed from the irradiated sample, which supports the feasibility of the strategy. The mean fluorescence intensity of the irradiated cells was approximately 50 times higher than that of nonirradiated cells with either NPC-biotin or DMNPE-biotin as the caged biotin, as determined by flow cytometry (Figure 4C; see also Figure S4A). As shown in Figure 4D, the rate of uncaging of DMNPE-biotin was slightly higher than that of NPC-biotin. The amounts of energy required to uncage half of the caged biotin were 0.24 J/cm^2 (NPC-biotin) and 0.17 J/cm^2 (DMNPE-biotin), respectively. The background fluorescence from streptavidin that bound to caged biotin without irradiation

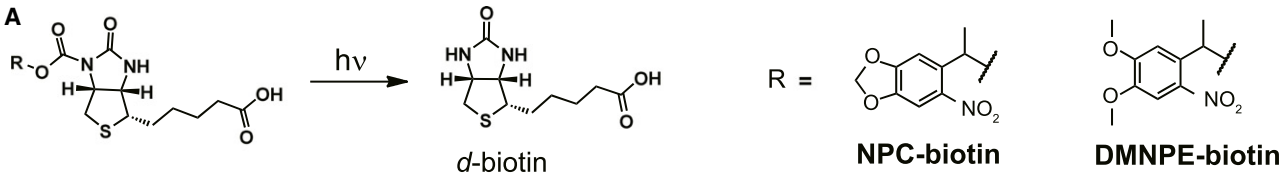

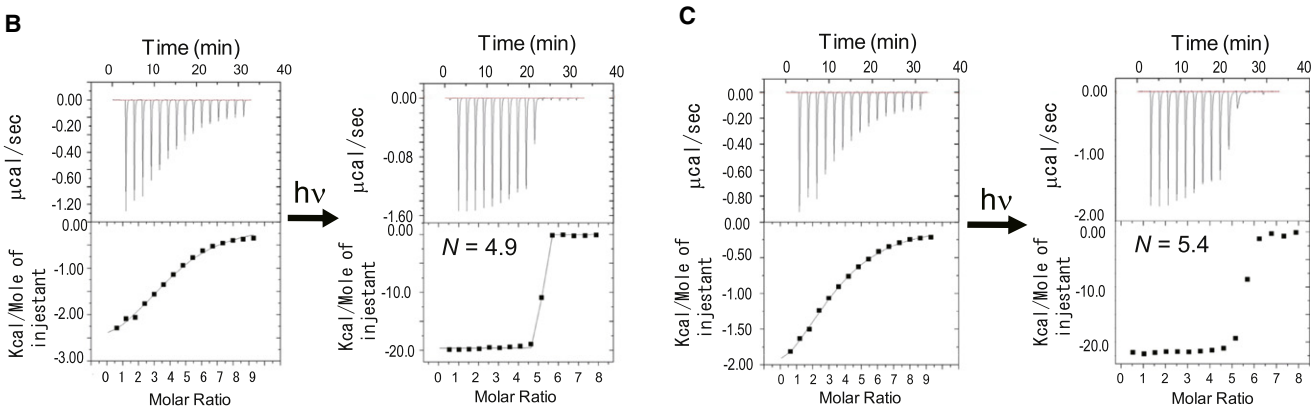

D

	N	K_a (M^{-1})	Δ*H* (cal/mol)	Δ*S* (cal/mol/deg)
NPC-biotin	4.1	1.5×10^4	-3.1×10^3	8.9
DMNPE-biotin	3.3	1.3×10^4	-2.7×10^3	9.9

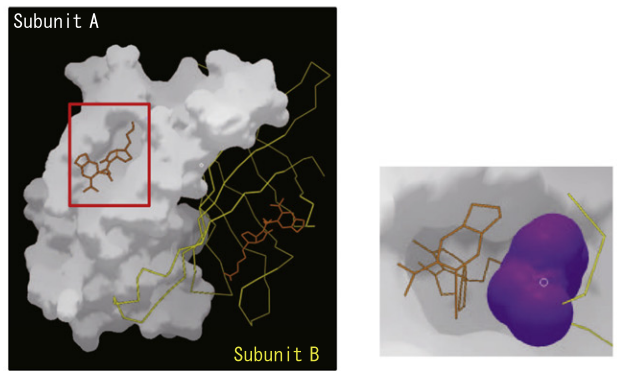

Figure 3. Development of Caged Biotins that Recover Full Affinity for Avidin Only after Photoirradiation

(A) Scheme of photodegradation process of caged biotins.

(B) ITC experiment with NPC-biotin before and after photoirradiation. Heat effects were recorded as a function of time during 15 successive 2 μl injections of 3.3 mM solution of NPC-biotin into the cell containing either 56 μM solution of avidin or buffer solution (as control). After irradiation of NPC-biotin solution for 20 min, heat effects were recorded again as a function of time during 15 successive 2 μl injections of 500 μM solution of the irradiated sample into the cell containing either 10 μM solution of avidin or buffer solution. Buffer conditions: 0.1 M sodium phosphate, 0.4% DMSO (pH 7.4).

(C) Isothermal titration calorimetry of DMNPE-biotin before and after photoirradiation. The experimental conditions were the same as described above.

(D) ITC parameters of caged biotins modified at the urea moiety.

(E) Overall structures of the complexes between NPC-biotin and avidin. In the figure, avidin subunit A is shown in white as a space-filling model, and subunit B in yellow as a Ca wire model. The biotin-binding pocket is highlighted by a red square. A closeup view of the interface between subunits A and C is also shown. Subunit C is shown in yellow as a Ca wire model. Trp110 of subunit C is shown in purple. Biotin is shown in red stick. Avidin is shown as a semitransparent surface, and the biotin pocket of avidin is highlighted.

See also Figures S1 and S3 and Table S1.

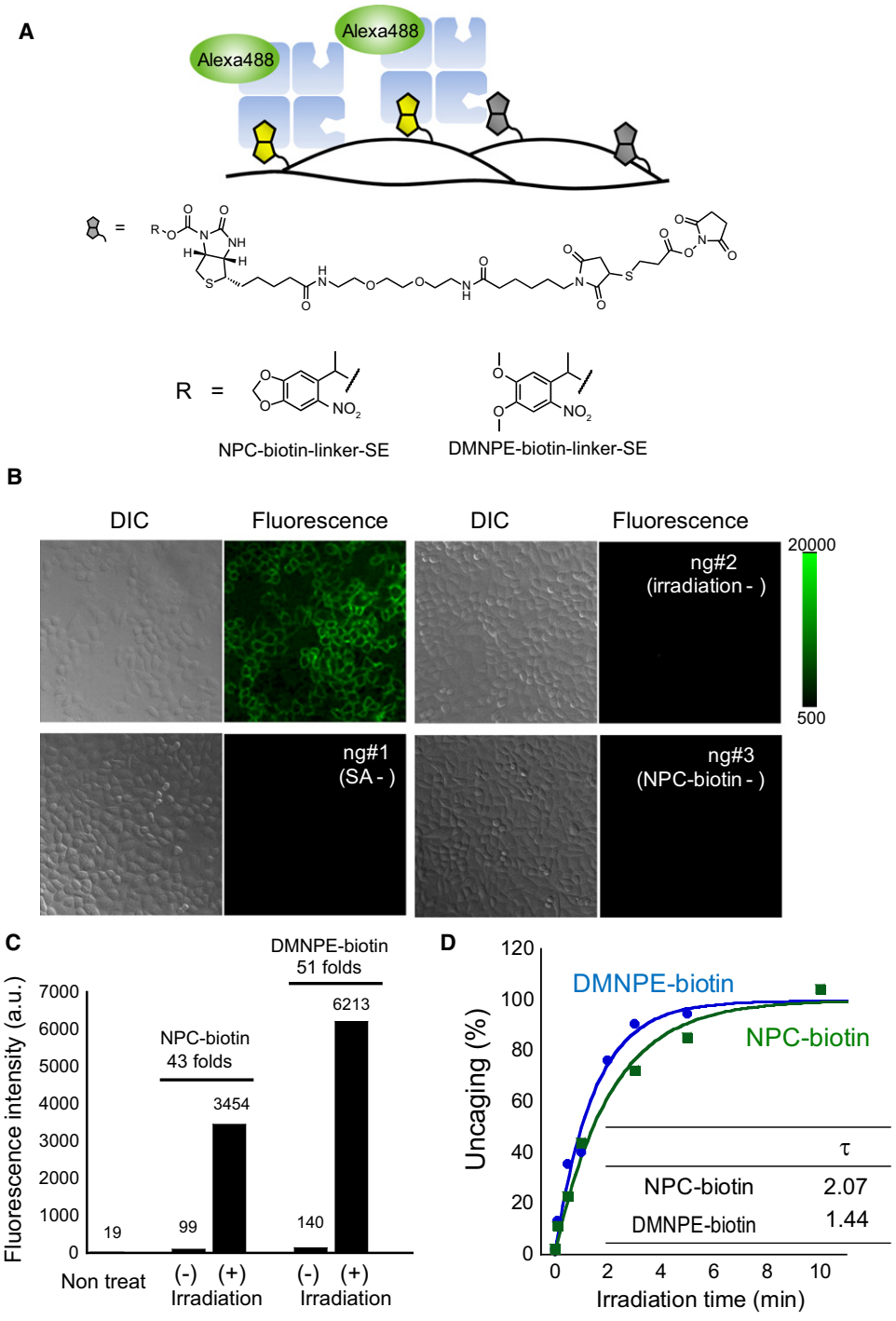

Figure 4. Specific Fluorescence Labeling of Irradiated Cells Using Caged Biotin Derivatives

(A) Strategy for specific fluorescence labeling of irradiated cells by combined use of streptavidin conjugated with a fluorophore and pretargeted caged biotin. The chemical structure of the labeling agent, caged biotin-linker-SE, is also shown.

(B) Epi-fluorescence and DIC images of HeLa cells that were labeled by NPC-biotin and subsequently treated with streptavidin-conjugated AlexaFluor488. Irradiation was performed for 5 min (2.8 mW/cm^2), before the addition of streptavidin-Alexa488. ng#1 to 3 represent control cells without streptavidin-Alexa488, light irradiation, and NPC-biotin, respectively.

(C) The mean fluorescence intensity of 10,000 cells treated with caged biotin, streptavidin-conjugated AlexaFluor488 and with/without irradiation, analyzed by flow cytometry.

(D) Relationship between irradiation time and the amount of bound streptavidin conjugated with AlexaFluor488. Uncaging rates were evaluated from the average fluorescence intensity from flow cytometric analysis, and the half reaction times (τ, min) are shown in the inset.

See also Figure S4.

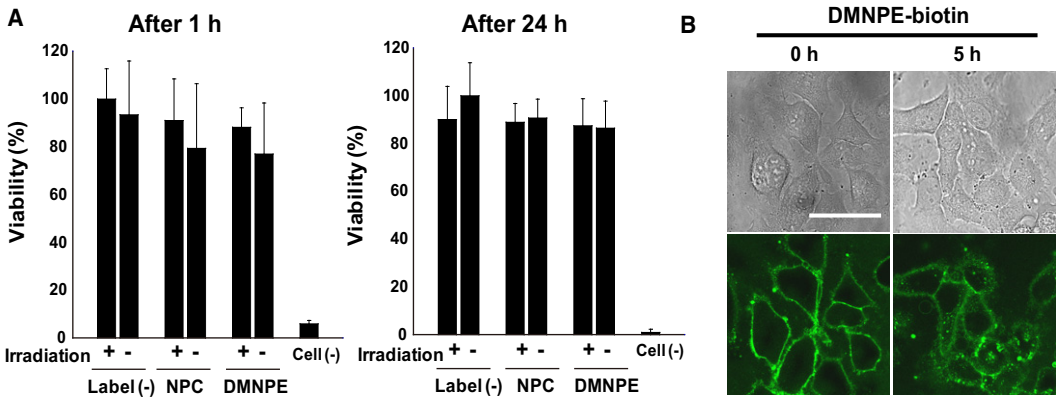

Figure 5. Cell Viability and Fluorophore Localization of Cells Labeled with Caged Biotin and Streptavidin Conjugated with AlexaFluor488

(A) Cell viability of HeLa cells treated with caged biotin, streptavidin, and light irradiation. The left figure shows the viability at 1 hr after the light irradiation. The right figure shows the viability at 24 hr after the light irradiation. The viability assays were performed with Cell Counting Kit-8 (CCK-8). The error bars indicate the standard deviation of eight independent experiments.

(B) Bright field (upper panel) and confocal fluorescence (lower panel) images of HeLa cells labeled with DMNPE-biotin and streptavidin-conjugated AlexaFluor488. The images were taken immediately after or 5 hr after the treatment. The size scale bar was 50 μm.

See also Figure S5.

was also determined. As shown in Figure 4C, NPC-biotin gave a weaker background signal than DMNPE-biotin, although the difference was not large. Considering both the efficiency of uncaging and the amount of background binding, we mainly used DMNPE-biotin for subsequent cellular applications. In Figure 4B, the result of whole-dish irradiation is shown for clarity, but of course, it was possible to label only cells of interest specifically in a single dish (Figure S4B).

One concern in using caged biotins is the possible cytotoxicity of the compounds, especially of the nitroso intermediate (Il'ichev et al., 2004), as well as that of UV light. Hence, the effect of the compounds themselves and the effect of irradiation were examined by means of CCK-8 cell survival assay, soon after the treatment and 24 hr later (Figure 5A). In both cases, caged biotin showed no significant toxicity, suggesting that it is possible to label live cells with caged biotin without causing severe damage. Confocal microscopy (Figure 5B; Figure S5) showed that the biotin/streptavidin complex remained localized on the cell surface immediately after the labeling and 5 hr later, although a part of the complex might have been transported inside cells within 5 hr. Taken together, these results indicate that it is feasible to use the caged biotin system to track cells for a period of at least several hours.

Application for Photoirradiated Cell-Specific Nuclear Staining

As a second application, we conceived an antibody-directed enzyme prodrug therapy (ADEPT)-like strategy (Dubowchik and Walker, 1999) for specific nuclear staining of irradiated cells, by combined use of streptavidin conjugated with β-galactosidase, Hoechst-Oβgal and pretargeted caged biotin (Figure 6A). Hoechst33258 is a nuclear staining fluorophore widely used in live cells (Figure 6B) (Breusegem et al., 2002). The compound, having cationic character and a planar aromatic system, interacts noncovalently with negatively charged double-stranded DNA or RNA by minor groove binding. Although the fluorescence of free Hoechst is extremely low in aqueous solution, when it binds to nucleic acids, a huge increase in fluorescence quantum yield occurs due to the stabilization of planar conformation (Barooah et al., 2011).

On the other hand, derivatives of the nuclear staining dyes that bear bulky substituents generally emit relatively weak fluorescence, presumably because of a less favorable binding to DNA (Koide et al., 2009). Therefore we derivatized Hoechst33258 with a bulky and hydrophilic β-galactoside moiety to yield an enzymatically activatable prodrug, Hoechst-Oβgal (Figure 6B; see also Figure S6A; see Supplemental Experimental Procedures for synthetic details), which exhibited a dramatic increase of fluorescence in live cells after hydrolysis by β-galactosidase. First, we confirmed that the fluorescence intensity of Hoechst was approximately 15 times higher than that of Hoechst-Oβgal in live cells (Figure 6C). Next, fluorescence images were captured after Hoechst-Oβgal loading of cells that had been incubated with NPC or DMNPE-biotin-linker-SE for 30 min, irradiated with a UV lamp, and mixed with streptavidin conjugated with β-galactosidase. The average fluorescence intensity of the cells exposed to photo-irradiation was higher than that without irradiation (4.4-fold for NPC-biotin, and 3.5-fold for DMNPE-biotin) (Figure 6D; see also Figure S6B). As compared with the contrast ratio of approximately 45-fold in the previous section, the values of the ratio in this experiment are not very satisfactory. A plausible factor is the presence of an unexpected background signal derived from the nonirradiated sample (Figure S6C), which suggests the presence of streptavidin conjugated with β-galactosidase that was nonspecifically bound to caged biotin on the cell surface. Analogous results were obtained using a fluorescent substrate of β-galactosidase, as well (Figures S6D and S6E).

Application for Photoirradiation-Specific Induction of Cell Death

As the third application, we developed a system of irradiated cell-specific induction of cell death by combined use of an anticancer prodrug, streptavidin conjugated with β-galactosidase, and pretargeted caged biotin (Figure 7A). We selected doxorubicin

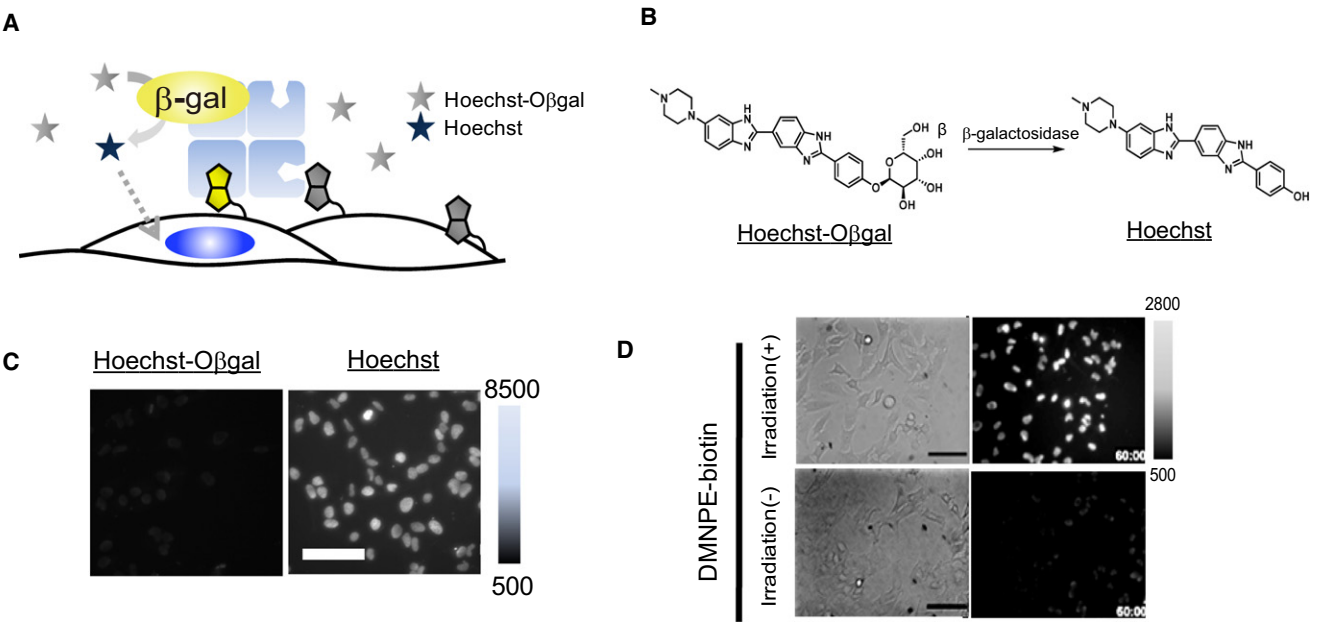

Figure 6. Photoirradiated Cell-Specific Nuclear Staining Using Hoechst-Oβgal

(A) Strategy for irradiated cell-specific nuclear staining by combined use of streptavidin conjugated with β-galactosidase and pretargeted caged biotin.

(B) Reaction scheme of Hoechst-Oβgal with β-galactosidase.

(C) Epi-fluorescence images of HeLa cells incubated with Hoechst-Oβgal (left) or native Hoechst (right). The size scale bar is 50 μm.

(D) DIC (left) and epi-fluorescence (right) images of HeLa cells treated with DMBPE-biotin, streptavidin conjugated with β-galactosidase, Hoechst-βgal, and with and without light irradiation. The size scale bar is 50 μm.

See also Figure S6.

(DXR), which is a widely used anticancer agent that works by intercalating DNA (Minotti et al., 2004), and is effective against proliferating cells. We synthesized a prodrug, DXR-βgal (Figure 7B), in which β-galactose and DXR are linked by a carbamate spacer (Devalapally et al., 2007) (see Supplemental Experimental Procedures for synthetic details). The IC_{50} of DXR-βgal was expected to be markedly larger than that of DXR itself, because the derivative should not interact with DNA, as discussed above for Hoechst-Oβal. Cytotoxicity assay was performed after incubation of the compounds for 24 hr, followed by an additional 24 hr incubation. The IC_{50} of DXR was calculated to be 79 nM while that of DXR-βgal was 13 μM (Figure S7). Next, to evaluate the induction of cell death using caged biotin, HeLa cells were incubated with caged-biotin-linker-SE for 30 min, illuminated with UV light, and incubated with streptavidin conjugated with β-galactosidase for 10 min. Then, DXR-βgal was loaded into the medium for 24 hr, and the cells were incubated for an additional 24 hr without the compound. As determined by CCK-8 assay, approximately 45% of the irradiated cells remained alive ($p < 0.01$ versus unirradiated cells by Student's t test), while no significant difference was observed between nonirradiated cells and control cells (Figure 7C). Although there is room for improvement as to the percentage of dead cells, it is clear that specific induction of cell death of photoirradiated cells was achieved.

DISCUSSION

Although (strept)avidin-biotin interaction is universally used in biology, it is not suitable for every application. For example, the dissociation constant of the order of 10^{-15} is too strong for affinity purification and very harsh conditions are required to elute the biotin-conjugated molecules, which sometimes leads to alteration of the native function or conformation of the targets. To solve this problem, two approaches have been mainly employed: mutation of the proteins and derivatization of biotin. In the former approach, avidin and streptavidin with a mutation at W110 and W120, respectively, were found to have lower binding affinity to biotin ($K_a \sim 10^8\ M^{-1}$). Interruption of intersubunit contacts was suggested to be the cause (Laitinen et al., 1999; Sano and Cantor, 1995), though no structural data were provided. The crystal structures in this study are the first structural data to demonstrate the importance of the Trp residue. As to the latter approach, several compounds, including desthiobiotin (Hirsch et al., 2002), 2-iminobiotin (Fudem-Goldin and Orr, 1990), and HABA (Green, 1970), which act as reversible binders to (strept)avidin, have been developed. Our results here suggest that introduction of substituents at N′-1 would be an alternative way to attenuate the binding affinity to realize reversible binding, because some of our compounds showed moderate affinity in the range of $K_a \sim 10^6\ M^{-1}$. Because the origin of the overwhelming binding affinity of the avidin-biotin complex has attracted attention in the fields of computational (Tong et al., 2010), medicinal (Kuhn and Kollman, 2000) and supermolecular (Rekharsky et al., 2007) chemistry, the present results should be of wide interest.

Another potential problem with native (strept)avidin-biotin complex is the multivalency, which might lead to aggregation or functional interference with molecules of interest. To address

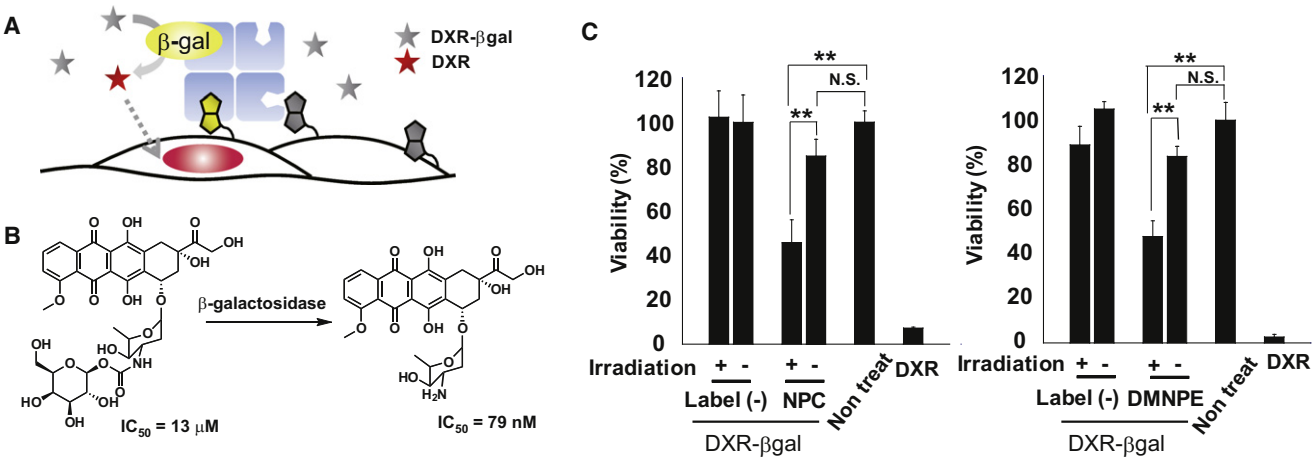

Figure 7. Application for Irradiated Cell-Specific Induction of Cell Death Using DXR-βgal

(A) Strategy for photoirradiated cell-specific induction of cell death by combined use of streptavidin conjugated with β-galactosidase and pretargeted caged biotin.

(B) Reaction scheme of DXR-βgal with β-galactosidase. IC_{50} values of DXR and DXR-βgal are shown under the structures.

(C) Cell viability of HeLa cells treated with caged biotin (left: NPC-biotin, right: DMNPC-biotin), streptavidin conjugated with β-galactosidase, DXR(-βgal) and with and without light irradiation. Error bars stand for the standard deviation of three independent experiments. **$p < 0.01$ by Student's t test. N.S., not significant. See also Figure S7.

this issue, monomeric (strept)avidin was developed by site-directed mutation (Laitinen et al., 2003; Qureshi and Wong, 2002; Howarth et al., 2006). Interestingly, the results of our ITC experiments shown in Figure 2 imply that only two monoZ-biotin molecules bind to avidin in solution, and this might provide a clue to allow the development of a monovalent avidin complex through the synthesis of novel biotin derivatives.

As noted above, the idea of caged biotin itself is not original to this work. However, biological application of caged biotin to cells, e.g., for site-specific fluorescence labeling and drug delivery, is unprecedented to our knowledge. As compared with caged fluorophores (Kobayashi et al., 2007), the fluorescence labeling system developed in this study has several advantages. First, fluorophores such as Alexa dyes, which do not possess hydroxyl or amino groups, as well as large fluorescent entities such as quantum dots, can be used. Second, by means of successive irradiation and incubation, it would be possible to achieve multicolor labeling. Third, in comparison with caged fluorophores, the streptavidin-conjugated fluorophores used in this strategy are more readily available.

For our last two applications, we selected β-galactosidase as the enzyme, because of its high catalytic turnover, stability, availability, and the established usage in reporter gene assay (Silverman et al., 1998) and ADEPT (Dubowchik and Walker, 1999). In biology and medicine, there is a huge demand to deliver chemicals only to selected cells/tissues. Various methodologies have been developed for this purpose, including a gene expression-dependent system (Greco and Dachs, 2001), an antibody-dependent system (Dubowchik and Walker, 1999), and an irradiation-dependent method (Ellis-Davies et al., 2007). Compared with them, the method introduced in this study has many advantages; for example, (1) it does not require troublesome transfection or expensive antibody, (2) active compounds can be catalytically produced, (3) spatial specificity even down to the single cell level could theoretically be obtainable, and (4) damage to the cells seems to be negligible. A remaining problem with the current system is the nonspecific binding of streptavidin conjugated with β-galactosidase to the surface of nontarget cells. Among various approaches that we tried to obviate this, washing with diluted acetic acid was most effective to decrease the background, but it may be possible to further reduce it by changing the enzyme or method of conjugation. It should also be pointed out that the suboptimal difference of cell survival between irradiated and unirradiated cells shown in Figure 7C is partially due to the cytotoxic activity of uncleaved DXR-βgal itself, so this issue might be overcome by the use of other drugs. Of course, lateral diffusion of the active molecule is an inherent drawback of all caged compounds, and this release system is no exception. However, we believe there may be ways to decrease the effect, including three-dimensional culture of cells.

Because this is the first study using caged biotins in live cells, the applications shown here represent proofs of concept, and may need further development. We would like to emphasize, however, that the scope of potential biological applications of caged biotin-streptavidin pairs is very wide. For instance, a variety of natural or synthetic molecules such as receptor agonists/antagonists, growth factors, chemokines, and MRI or PET imaging agents, could be specifically localized on the surface of cells of interest, to decipher the complex machinery of living systems. We hope that this study will provide the stimulus for developing a broad range of applications of caged biotins.

SIGNIFICANCE

We investigated in detail the affinity for avidin of biotin derivatives modified at the urea moiety, and found for the first time that modification at this site generally reduced the affinity by 10^9∼10^{10}-fold, compared with native biotin. The X-ray structures of these complexes were solved, and

the results suggested that the modification perturbs both the electrostatic and hydrophobic interactions of the protein and ligand. Based on the results, we developed photoreleasable caged biotins that could be used to label the surface of live cells.

To demonstrate the utility of these compounds, we carried out site-specific fluorescence labeling of cultured cells with high contrast, by means of photoirradiation of cells labeled with caged biotin in the presence of streptavidin-conjugated fluorophores. Moreover, we successfully demonstrated nuclear staining and induction of cell death specifically in photo-irradiated cells. In combination with other kinds of fluorophores, biologically active compounds, or enzymes, these biotin derivatives should serve as potentially useful tools in various fields of biology.

EXPERIMENTAL PROCEDURES

Protein Crystallization

Avidin from egg white was purchased from Wako Pure Chemical Industries. Avidin was crystallized at a protein concentration of 10 mg/ml by the sitting-drop vapor method in 2.5–2.7 M ammonium sulfate with 0.1 M sodium citrate (pH 4.0–5.0) with continuous stirring (Adachi et al., 2004). The protein solutions were crystallized at 293 K, and the crystal growth vessels (Hampton Research) were covered with 0.08 mm thick sealing tape (JT Science). The volume of the protein drops was 2 μl.

X-Ray Diffraction

X-ray diffraction experiments were performed under liquid-nitrogen-cooled conditions at 100 K. An avidin crystal was mounted in a nylon loop, soaked briefly in cryoprotectant solution and then frozen by rapidly submerging it in liquid nitrogen. X-ray diffraction data were collected at beamline BL44XU of the SPring-8 synchrotron-radiation source (Harima, Japan). Diffraction data were processed and scaled using HKL-2000. The data collection and processing statistics are summarized in Table S1.

Structure Determinations and Refinements

The deposited structure coordinates for avidin P42212 form crystal (PDB ID code 1AVD) were used as a starting model for the structural analysis. Structural refinements were carried out using a stereochemically constrained least-squares refinement method in the CNS program package and Refmac software (Murshudov et al., 1999) as implemented within the CCP4 package (Collaborative Computational Project, Number 4, 1994). Refinement statistics are depicted in Table S1.

ITC Analysis

Isothermal titration calorimetry experiments were carried out with an ITC200 (Microcal, Inc.). Calorimeters were electrically calibrated according to the manufacturer's instructions. Protein or a chemical compound was loaded into the calorimeter cell as described in the text. The titration syringe was loaded with another reactant at 10- to 20-fold greater concentration than in the cell. Titrations were usually carried out using 10–15 injections of 15 μl or 10 μl each injected at 150 s intervals. Stirring was performed at 1000 rpm as suggested by the manufacturer. Titrations were carried out at 30°C. Both reactants were dissolved in the same solution containing 100 mM sodium phosphate (pH 7.4), as described in the text.

Flow Cytometric Analysis

HeLa cells (1×10^5 cells/ml) were cultured overnight in DMEM on a 35 mm glass-bottomed cell culture dish (Matsunami Corp.). The medium was removed after 24 hr, and the cells were washed three times with 1 ml of PBS. Then a Hank's balanced salt solution (HBSS) buffer (Invitrogen Corp.) (700 μl) containing 5 μM NPC or DMNPE-biotin-linker SE (0.1% DMSO as a cosolvent) was added and the cells were incubated for 30 min at 37°C. The cells were then washed twice with PBS (1 ml), and illuminated with a high-pressure UV lamp (SLUV-4, Asone) at 365 nm. After illumination, 2 μM streptavidin conjugated with AlexaFluor 488 in 1 ml of HBSS was added and the cells were incubated for 10 min at room temperature. After having been washed twice with PBS (1 ml), the cells were trypsinized, pelleted, resuspended in DMEM and, if necessary, the cell suspensions were mixed. Then the fluorescence of the cells was analyzed by a BD LSR II flow cytometer (Becton Dickinson). Every experiment was done several times.

Epi-Fluorescence Imaging of Specific Fluorescence Labeling of Irradiated Cells

HeLa cells (1×10^5 cells/ml) were cultured on a 35 mm glass-bottomed cell culture dish (Matsunami Corp.) and cultured overnight in DMEM. The medium was removed after 24 hr, and the cells were washed three times with 1 ml of PBS. Then a Hank's balanced salt solution (HBSS) buffer (Invitrogen Corp.) (700 μl) containing 20 μM NPC or DMNPE-biotin-linker SE (0.1% DMSO as a cosolvent) was added and the cells were incubated for 30 min at 37°C. The cells were then washed twice with PBS (1 ml), and illuminated with a high-pressure mercury lamp (BH2-RFL-T3, Olympus) via a 330–385 nm band-pass filter (BP330-385, Olympus) through the objective lens (UPlanFL N 40×, Olympus) of a fluorescence microscope (IX71, Olympus). After illumination, 6 μM streptavidin conjugated with AlexaFluor 488 in 1 ml of HBSS was added and the cells were incubated for 10 min at room temperature. The cells were then washed twice with PBS (1 ml), and the fluorescence images were acquired with an IX71 imaging system (Olympus) equipped with a cooled CCD camera (Coolsnap HQ, Photometrics), using a xenon lamp (AH2-RX-T, Olympus) with a BP 470-490 excitation filter and a BA 510–550 emission filter. Every experiment was done twice.

Confocal Imaging of Specific Fluorescence Labeling of Irradiated Cells

Essentially the same procedure as above was employed. We used a confocal imaging system (TCS-SP5X; Leica) equipped with a white light laser. Fluorescence images were captured using a Leica Application Suite Advanced Fluorescence (LAS-AF) with a 10× objective lens. The excitation wavelength was 488 nm and emission was collected in the range of 510–550 nm.

Cytotoxicity Assay

HeLa cells (5×10^3 cells/well) were cultured overnight in DMEM on a 96-well plate (Thermo Scientific, AB-1100/k). The medium was removed after 24 hr, and the cells were washed three times with PBS. Then a Hank's balanced salt solution (HBSS) buffer (Invitrogen Corp.) (100 μl) containing 5 μM NPC or DMNPE-biotin-linker SE (0.1% DMSO as a cosolvent) was added and the cells were incubated for 30 min at 37°C. The cells were then washed twice with PBS, and illuminated with a UV lamp (SLUV-4, Asone) at 365 nm. After illumination, 6 μM streptavidin in HBSS was added and the cells were incubated for 10 min at room temperature. The cells were then washed with PBS, 0.1% acetic acid solution, and PBS, successively. The irradiated cells were incubated for 24 hr after treatment and the medium was replaced with 100 μl of DMEM containing 10% Cell Counting Kit-8 (DOJINDO). Cells were incubated for another 1–4 hr and the absorbance at 440 nm was measured using a SH-8000 plate reader (Corona Electric). Absorbance at 650 nm was also measured and the value was subtracted as the background. Values of the wells containing cells without biotin derivatives, streptavidin or light treatment was set as corresponding to fully alive, and values of the wells without cells were set as blank. Every experiment was done several times.

Cell Assay with Hoechst-Oβgal

HeLa cells (1×10^5 cells/ml) were cultured overnight in DMEM on a 35 mm glass-bottomed cell culture dish (Matsunami Corp.). The medium was removed after 24 hr, and the cells were washed three times with 1 ml of PBS. Then a Hank's balanced salt solution (HBSS) buffer (Invitrogen Corp.) (700 μl) solution containing 5 μM NPC or DMNPE-biotin-linker SE (0.1% DMSO as a cosolvent) was added and the cells were incubated for 30 min at 37°C. The cells were then washed twice with PBS (1 ml), and illuminated with a UV lamp (SLUV-4, Asone) at 365 nm. After illumination, 600 nM streptavidin conjugated with β-galactosidase in 1 ml of HBSS was added and the cells were incubated for 10 min at room temperature. Then the cells were washed with PBS, 0.1% acetic acid, and PBS, successively. Hoechst or

Hoechst-Oβgal (20 μM, 1 ml) was added and fluorescence images were acquired with anIX71 imaging system (Olympus, Japan) equipped with a cooled CCD camera (Coolsnap HQ, Photometrics), using a xenon lamp (AH2-RX-T, Olympus) with a BP 330–385 excitation filter and a BP 460–495 emission filter. Every experiment was done several times.

Cell Assay with DXR-βgal

HeLa cells (5×10^3 cells/well) were cultured overnight in DMEM on a 96-well plate (Thermo Scientific, AB-1100/k). The medium was removed after 24 hr, and the cells were washed twice with PBS. Then a Hank's balanced salt solution (HBSS) buffer (100 μl) solution containing 5 μM NPC or DMNPE-biotin-linker SE (0.1% DMSO as a cosolvent) was added and the cells were incubated for 30 min at 37°C in the dark. The cells were then washed twice with PBS, and illuminated with a mercury handy UV lamp at 365 nm. After illumination, streptavidin conjugated with β-galactosidase (0.6 μM, 100 μl) in HBSS was added and the cells were incubated for 10 min at room temperature. The cells were then washed with PBS, 0.1% acetic acid, and PBS again. Doxorubicin or doxorubicin-βgal (10 μM, 100 μl) in HBSS was added to the medium and the cells were incubated for 24 hr. After the treatment, the cells were incubated for another 24 hr, then the medium was replaced with 100 μl of DMEM containing 10% Cell Counting Kit-8 (DOJINDO). Cells were incubated for another 1–4 hr and the absorbance at 440 nm was measured using a SH-8000 plate reader (Corona Electric Co., Ltd.). Absorbance at 650 nm was also measured and the value was subtracted as the background. Values of the wells containing cells without biotin derivatives, streptavidin, or light treatment was set as corresponding to fully alive, and values from the wells without cells were set as blank. Every experiment was done several times.

ACCESSION NUMBERS

The coordinates of the X-ray crystal structures of monoZ-biotin, monoAc-biotin, diMe-biotin, and NPC-biotin in complex with avidin have been deposited to the PDB (http://www.rcsb.org) under accession codes 3VHI, 3VGW, 3VHH, and 3VHM, respectively.

SUPPLEMENTAL INFORMATION

Supplemental Information includes seven figures, one table, and Supplemental Experimental Procedures and can be found with this article online at doi:10.1016/j.chembiol.2011.09.007.

ACKNOWLEDGMENTS

The authors thank Yukio Tada for computer modeling of protein complexes, Masanori Osawa and Nae Saito for the ITC experiment, Eiki Yamashita, Yasufumi Umena, Masato Yoshimura, and Atsushi Nakagawa for support during data collection at SPring-8 beamline 44XU, and Yasuteru Urano, Kenjiro Hanaoka, Tasuku Ueno and Toru Komatsu for helpful discussions. This work was supported in part by the Ministry of Education, Culture, Sports, Science and Technology of Japan (grant nos. 22000006 to T.N., and 23651231 to T.T.), and by a grant from the New Energy and Industrial Technology Development Organization (NEDO) of Japan (to T.T.). T.T. was also supported by the Cosmetology Research Foundation, Japan.

Received: June 2, 2011
Revised: August 1, 2011
Accepted: September 10, 2011
Published: October 27, 2011

REFERENCES

Adachi, H., Matsumura, H., Niino, A., Takano, K., Kinoshita, T., Warizaya, M., Inoue, T., Mori, Y., and Sasaki, T. (2004). Improving the quality of protein crystals using stirring crystallization. Jpn. J. Appl. Phys. *43*, L522–L525.

Barooah, N., Mohanty, J., Pal, H., Sarkar, S.K., Mukherjee, T., and Bhasikuttan, A.C. (2011). pH and temperature dependent relaxation dynamics of Hoechst-33258: a time resolved fluorescence study. Photochem. Photobiol. Sci. *10*, 35–41.

Breusegem, S.Y., Clegg, R.M., and Loontiens, F.G. (2002). Base-sequence specificity of Hoechst 33258 and DAPI binding to five $(A/T)_4$ DNA sites with kinetic evidence for more than one high-affinity Hoechst 33258-AATT complex. J. Mol. Biol. *315*, 1049–1061.

Collaborative Computational Project, Number 4. (1994). The CCP4 suite: programs for protein crystallography. Acta Crystallogr. D Biol. Crystallogr. *50*, 760–763.

Devalapally, H., Navath, R.S., Yenamandra, V., Akkinepally, R.R., and Devarakonda, R.K. (2007). β-galactoside prodrugs of doxorubicin for application in antibody directed enzyme prodrug therapy/prodrug monotherapy. Arch. Pharm. Res. *30*, 723–732.

Diamandis, E.P., and Christopoulos, T.K. (1991). The biotin-(strept)avidin system: principles and applications in biotechnology. Clin. Chem. *37*, 625–636.

Dubowchik, G.M., and Walker, M.A. (1999). Receptor-mediated and enzyme-dependent targeting of cytotoxic anticancer drugs. Pharmacol. Ther. *83*, 67–123.

Ellis-Davies, G.C.R. (2007). Caged compounds: photorelease technology for control of cellular chemistry and physiology. Nat. Methods *4*, 619–628.

Ellis-Davies, G.C.R., Matsuzaki, M., Paukert, M., Kasai, H., and Bergles, D.E. (2007). 4-Carboxymethoxy-5,7-dinitroindolinyl-Glu: an improved caged glutamate for expeditious ultraviolet and two-photon photolysis in brain slices. J. Neurosci. *27*, 6601–6604.

Fudem-Goldin, B., and Orr, G.A. (1990). 2-Iminobiotin-containing reagent and affinity columns. Methods Enzymol. *184*, 167–173.

Gee, K.R., Carpenter, B.K., and Hess, G.P. (1998). Synthesis, photochemistry, and biological characterization of photolabile protecting groups for carboxylic acids and neurotransmitters. Methods Enzymol. *291*, 30–50.

Greco, O., and Dachs, G.U. (2001). Gene directed enzyme/prodrug therapy of cancer: historical appraisal and future prospectives. J. Cell. Physiol. *187*, 22–36.

Green, N.M. (1963). Avidin 1. The use of [^{14}C] biotin for kinetic studies and for assay. Biochem. J. *89*, 585–591.

Green, N.M. (1970). Spectrophotometric determination of avidin and biotin. Methods Enzymol. *18*, 418–424.

Hengsakul, M., and Cass, A.E.G. (1996). Protein patterning with a photoactivatable derivative of biotin. Bioconjug. Chem. *7*, 249–254.

Hirsch, J.D., Eslamizar, L., Filanoski, B.J., Malekzadeh, N., Haugland, R.P., Beechem, J.M., and Haugland, R.P. (2002). Easily reversible desthiobiotin binding to streptavidin, avidin, and other biotin-binding proteins: uses for protein labeling, detection, and isolation. Anal. Biochem. *308*, 343–357.

Howarth, M., Chinnapen, D.J.-F., Gerrow, K., Dorrestein, P.C., Grandy, M.R., Kelleher, N.L., El-Husseini, A., and Ting, A.Y. (2006). A monovalent streptavidin with a single femtomolar biotin binding site. Nat. Methods *3*, 267–273.

Il'ichev, Y.V., Schwörer, M.A., and Wirz, J. (2004). Photochemical reaction mechanisms of 2-nitrobenzyl compounds: methyl ethers and caged ATP. J. Am. Chem. Soc. *126*, 4581–4595.

Kim, K., Yang, H., Jon, S., Kim, E., and Kwak, J. (2004). Protein patterning based on electrochemical activation of bioinactive surfaces with hydroquinone-caged biotin. J. Am. Chem. Soc. *126*, 15368–15369.

Kobayashi, T., Urano, Y., Kamiya, M., Ueno, T., Kojima, H., and Nagano, T. (2007). Highly activatable and rapidly releasable caged fluorescein derivatives. J. Am. Chem. Soc. *129*, 6696–6697.

Koide, Y., Urano, Y., Yatsushige, A., Hanaoka, K., Terai, T., and Nagano, T. (2009). Design and development of enzymatically activatable photosensitizer based on unique characteristics of thiazole orange. J. Am. Chem. Soc. *131*, 6058–6059.

Kuhn, B., and Kollman, P.A. (2000). Binding of a diverse set of ligands to avidin and streptavidin: an accurate quantitative prediction of their relative affinities by a combination of molecular mechanics and continuum solvent models. J. Med. Chem. *43*, 3786–3791.

Laitinen, O.H., Airenne, K.J., Marttila, A.T., Kulik, T., Porkka, E., Bayer, E.A., Wilchek, M., and Kulomaa, M.S. (1999). Mutation of a critical tryptophan to lysine in avidin or streptavidin may explain why sea urchin fibropellin adopts an avidin-like domain. FEBS Lett. *461*, 52–58.

Laitinen, O.H., Nordlund, H.R., Hytönen, V.P., Uotila, S.T.H., Marttila, A.T., Savolainen, J., Airenne, K.J., Livnah, O., Bayer, E.A., Wilchek, M., and Kulomaa, M.S. (2003). Rational design of an active avidin monomer. J. Biol. Chem. *278*, 4010–4014.

Lee, K.B., Park, S.J., Mirkin, C.A., Smith, J.C., and Mrksich, M. (2002). Protein nanoarrays generated by dip-pen nanolithography. Science *295*, 1702–1705.

Lin, S., Hanson, R.E., and Cronan, J.E. (2010). Biotin synthesis begins by hijacking the fatty acid synthetic pathway. Nat. Chem. Biol. *6*, 682–688.

McMahon, R.J., ed. (2008). Avidin-Biotin Interactions Methods and Applications, Methods in Mol. Biol., 418 (New York: Humana Press).

Minotti, G., Menna, P., Salvatorelli, E., Cairo, G., and Gianni, L. (2004). Anthracyclines: molecular advances and pharmacologic developments in antitumor activity and cardiotoxicity. Pharmacol. Rev. *56*, 185–229.

Murshudov, G.N., Vagin, A.A., Lebedev, A., Wilson, K.S., and Dodson, E.J. (1999). Efficient anisotropic refinement of macromolecular structures using FFT. Acta Crystallogr. D Biol. Crystallogr. *55*, 247–255.

Pazy, Y., Kulik, T., Bayer, E.A., Wilchek, M., and Livnah, O. (2002). Ligand exchange between proteins. Exchange of biotin and biotin derivatives between avidin and streptavidin. J. Biol. Chem. *277*, 30892–30900.

Pirrung, M.C., and Huang, C.-Y. (1996). A general method for the spatially defined immobilization of biomolecules on glass surfaces using "caged" biotin. Bioconjug. Chem. *7*, 317–321.

Pugliese, L., Coda, A., Malcovati, M., and Bolognesi, M. (1993). Three-dimensional structure of the tetragonal crystal form of egg-white avidin in its functional complex with biotin at 2.7 A resolution. J. Mol. Biol. *231*, 698–710.

Qureshi, M.H., and Wong, S.-L. (2002). Design, production, and characterization of a monomeric streptavidin and its application for affinity purification of biotinylated proteins. Protein Expr. Purif. *25*, 409–415.

Rekharsky, M.V., Mori, T., Yang, C., Ko, Y.H., Selvapalam, N., Kim, H., Sobransingh, D., Kaifer, A.E., Liu, S.M., Isaacs, L., et al. (2007). A synthetic host-guest system achieves avidin-biotin affinity by overcoming enthalpy-entropy compensation. Proc. Natl. Acad. Sci. USA *104*, 20737–20742.

Sakahara, H., and Saga, T. (1999). Avidin-biotin system for delivery of diagnostic agents. Adv. Drug Deliv. Rev. *37*, 89–101.

Sano, T., and Cantor, C.R. (1995). Intersubunit contacts made by tryptophan 120 with biotin are essential for both strong biotin binding and biotin-induced tighter subunit association of streptavidin. Proc. Natl. Acad. Sci. USA *92*, 3180–3184.

Shimizu, N., Sugiyama, S., Maruyama, M., Yoshikawa, H.Y., Takahashi, Y., Adachi, H., Takano, K., Murakami, S., Inoue, T., Matsumura, H., and Mori, Y. (2009). Growth of large protein crystals by top-seeded solution growth together with the floating and solution-stirring technique. Cryst. Growth Des. *9*, 5227–5232.

Silverman, L., Campbell, R., and Broach, J.R. (1998). New assay technologies for high-throughput screening. Curr. Opin. Chem. Biol. *2*, 397–403.

Stanley, J.S., Griffin, J.B., and Zempleni, J. (2001). Biotinylation of histones in human cells. Effects of cell proliferation. Eur. J. Biochem. *268*, 5424–5429.

Sugawara, K., Hoshi, S., Akatsuka, K., Tanaka, S., and Nakamura, H. (1997). Effect of the steric hindrance and alkyl chain of a biotin derivative to avidin-biotin binding. Anal. Sci. *13*, 677–679.

Sundberg, S.A., Barrett, R.W., Pirrung, M., Lu, A.L., Kiangsoontra, B., and Holmes, C.P. (1995). Spatially-addressable immobilazion of macromolecules on solid supports. J. Am. Chem. Soc. *117*, 12050–12057.

Tong, Y., Mei, Y., Li, Y.L., Ji, C.G., and Zhang, J.Z.H. (2010). Electrostatic polarization makes a substantial contribution to the free energy of avidin-biotin binding. J. Am. Chem. Soc. *132*, 5137–5142.

Wilchek, M., and Bayer, E.A. (1988). The avidin-biotin complex in bioanalytical applications. Anal. Biochem. *171*, 1–32.

Yamaguchi, S., Chen, Y., Nakajima, S., Furuta, T., and Nagamune, T. (2010). Light-activated gene expression from site-specific caged DNA with a biotinylated photolabile protection group. Chem. Commun. (Camb.) *46*, 2244–2246.

